

Dynamical impacts of convection and stochastic approaches

Glenn Shutts

*ECMWF, Shinfield Park, Reading
RG2 9AX, United Kingdom
glenn.shutts@ecmwf.int*

ABSTRACT

Some basic dynamical concepts concerning the interaction of convection with the large-scale flow are reviewed and their significance for numerical weather prediction and climate models is discussed. The interplay of deep convective mass transfer and the Earth's rotation enables the capture of buoyant energy in balanced flow phenomena such as mesoscale vortices. These flow systems are characterised by anomalous potential vorticity distributions which participate in the balanced flow dynamics that underpin the weather prediction problem. Convection may also excite gravity wave motions that cause self-organization in convective cloud systems such as the equatorially-trapped convectively-coupled Kelvin waves. The underlying sensitivity of convective initiation to dynamical and topographic forcing implies a level of unpredictability that may have to be treated by stochastic methods. The inability of current global weather prediction models to resolve the upscale energy transfers associated with deep convective systems compounds the problem. Attempts to address these issues with stochastic backscatter parametrization will be described.

1 Introduction

In this seminar the intention is to focus on the dynamical interaction of deep convection with the larger scale rotating and stratified environment and ignore cloud microphysical and radiative processes. However, the moist process and the release of latent heat energy is an essential part of deep, penetrative convection which involves the transfer of mass through a stably-stratified environment until a level of neutral buoyancy is found. At a more fundamental level, the stably-stratified troposphere is largely a consequence of the moist process (particularly in the tropics) since convection drives the atmosphere toward a state of moist convective neutrality (or *slantwise* convective neutrality, Korty and Schneider, 2007). This adjustment process is highly intermittent in time and insufficient to remove all of the Convective Available Potential Energy over large areas of the tropical oceans. Over continents in summer, upper level troughs and frontal systems can destabilize the troposphere and generate intense Mesoscale Convective Systems (MCSs). These are of sufficient scale and intensity to perturb the upper level westerlies and influence weather predictability.

In general the interaction of deep convection with the large-scale has been treated as a thermodynamic one within the context of convection parametrization for Numerical Weather Prediction (NWP) and climate models. These parametrization schemes have sought to describe the statistical equilibrium thermodynamic response of an ensemble of convective clouds under prescribed forcing. The dynamical influence of convective clouds in parametrization has usually been treated as a vertical mixing process i.e. 'cumulus friction' and modelling studies (e.g. Kershaw and Gregory, 1997) have shown the usefulness of such an approach. More controversial is the possible effect of horizontal mixing by collections of deep cumulonimbus clouds. Scorer (1966) proposed that the cumulonimbus clouds occurring in the circulation of a hurricane would mix angular momentum downgradient so as to increase the tangential velocity near the core of the hurricane. These ideas provoked much controversy in the late 1960s regarding the effect of turbulence in a rotating environment. Whereas viscosity would always tend to adjust the tangential velocity field to a deformation-free solid rotation state, turbulence might behave differently and actually force rotating flows. Gough and Lyndon-Bell (1968) proposed a 'vorticity-expulsion' hypothesis whereby turbulence would act to scramble the vortex lines associated with

solid-rotation flow and effectively push the mean vorticity to the edge of the turbulent region. They performed the famous ‘Alka Seltzer experiment’ where the bubbles released from indigestion tablets acted as stirring agents in a rotating beaker of water. Their results appeared to support the vorticity expulsion hypothesis. Of course, the behaviour of vortex lines in homogeneous turbulence is very different from that in stratified flows where baroclinic vorticity generation plays a vital role. More recent theories of hurricane formation *do* emphasize the role of convectively-generated eddies that effectively re-distribute angular momentum during the process of axisymmetrization (Montgomery and Kallenbach, 1997).

Clouds are naturally turbulent phenomena that entrain environmental air as they ascend. Intense vortex sheets form at the cloud boundaries due to the baroclinic generation of horizontal vorticity and these are highly unstable and tend to wind-up with environmental air to form ‘Swiss roll’ structures. However under certain conditions (e.g. large CAPE and very moist atmosphere) air may ascend rapidly to the upper troposphere with relatively little mixing. This permits the use of the inviscid flow assumption that facilitates various mathematical models of penetrative convection and which makes the use of conceptual flow diagrams meaningful (e.g. Browning and Ludlam, 1962). Parcel models ignore mixing and can be used for instance to define CAPE and to compute the balanced endstate after convection has taken place (see section 2). As will be shown this provides useful insights into the Potential Vorticity (PV) footprint left by MCSs and hurricanes.

Rarely, it is possible to arrive at closed analytic models that represent important aspects of convection. Moncrieff and Green (1972) describe an ingenious model of a steady, propagating convective storm which mathematically takes the form of a nonlinear, eigenvalue problem. They obtain a Lagrangian integral of the 2D horizontal vorticity equation (including the baroclinic generation term with pseudo-heat source) and solve this for an overturning sheared flow. The model (together with later models e.g. Moncrieff, 1981 and 1992) show the potential for upgradient momentum transport in squall line systems that have similar persistence and propagating characteristics.

The mechanisms by which kinetic energy released in deep convection finds its way upscale has been the subject of much interest, particularly in recent years in connection with stochastic backscatter parametrization. Kinetic energy created by buoyancy may be dissipated by turbulence, radiated away as gravity waves and captured in balanced flows. Most relevant to the NWP problem is the latter by virtue of its influence on weather system PV dynamics. Lilly (1983) hypothesized that convective outflow anvils behave like collapsing turbulent wakes for which a small fraction of the energy would escape upscale as part of a quasi-2D inverse energy cascade. 3D numerical simulations of deep convection by Vallis et al (1997) were aimed at quantifying the production of quasi-2D balanced flow and its upscale energy cascade. Although the $k^{-5/3}$ energy spectrum characteristic of the upscale energy-cascade for 2D turbulence was seen to emerge, the rate of transfer seemed quite small. The presence of ambient vorticity - either in the Earth’s rotation or in vertical wind shear - was seen to improve the effectiveness of the upscale energy transfer process though.

Gravity wave radiation from convection affects the large-scale flow through wave radiation stresses and although their influence is generally rather small in the troposphere, their impact in the stratosphere and mesosphere can be very large (e.g. in forcing the Quasi-Biennial Oscillation, Baldwin et al, 2001). In the tropics, deep convection couples closely with Kelvin waves (an eastward-propagating gravity wave with geostrophic zonal wind) whilst radiating energy into the stratosphere. For reasons that are not clearly understood, NWP models have difficulty representing the interaction between parametrized convection and Kelvin waves which appear to have their energy source located near the typical height of cloud top (i.e. ~ 250 hPa; see Shutts, 2008)

2 Parcel model of convection and equilibrium states

Since convection in the atmosphere involves the transport of mass from one level to the other in relatively narrow plumes it has been convenient to adopt the idea of ‘air parcel’ and environment. In the parcel approach a discrete lump of air is imagined to be able to move through the atmosphere without disturbing the environment. The buoyancy force is then related to the temperature difference between parcel and environment as

on a tephigram and perturbation pressure gradient forces are ignored in the vertical momentum equation. A buoyant air parcel then has a stable equilibrium point where the temperature of the parcel equals that of the environment. Bjerknes (1938) found a way of approximately accounting for the effects of forced subsidence in the environment close to ascending convective towers (the ‘slice method’).

In a simpler context one can view the atmosphere as composed of a stack of air parcels characterized by specific values of potential temperature with increasing values as one goes upward. (Fig. 1; left column). Given a surface pressure (fixed by the total mass of the parcels) it is possible to use hydrostatic balance to determine the distribution of density with height and therefore the gravitational potential energy. If one imagines that the lowest parcel is close to saturation and is lifted so that it releases latent heat and then ascends to find a new equilibrium position higher up, it is possible to determine a new equilibrium arrangement with monotonically increasing potential temperature (θ) with height (Fig. 1; right column). Parcels between the initial and final positions of the convecting parcel will be displaced downwards by the convecting parcel. The difference between the initial and final *static energy* of the column will be equal to the kinetic energy released (the details of this energy calculation are left to the reader to contemplate).

The above thought experiment replaces the concept of parcel buoyancy and environment with a single parcel rearrangement problem. The convective stability requirement that air parcels are arranged in increasing θ with height coupled with mass continuity dictates the thermodynamic profile. For a rotating system this parcel model can be extended to account for *inertial stability* which requires that the absolute vorticity ($f + \zeta$) measured on an isentropic surface is the same sign as the Coriolis parameter (f). If we consider a rectilinear flow directed in the y direction of a Cartesian system then:

$$f + \zeta = f + \frac{\partial v}{\partial x} = \frac{\partial M}{\partial x} \quad (1)$$

where v is the y -component of velocity and $M = fx + v$ is the absolute momentum. Differentiation with respect to x in eq.(1) is understood to be along constant θ surfaces. Inertial stability therefore requires that $\frac{\partial M}{\partial x} > 0$ in an analogous way to $\frac{\partial \theta}{\partial z} > 0$ implying dry convective stability. The parcel model can then be generalized with each parcel being characterized by constant values of M and θ but now the rearrangement problem involves organizing the parcels in the $x - z$ plane with increasing θ upwards and increasing M towards the right. A major additional complication is that the geometry of the parcels is now not rectangular in general and in fact can be any convex polygon. It can be shown however that if each parcel is characterized by a fixed area (i.e. the incompressibility assumption), and the sum of the areas of the parcels equals the area of the convex domain they must occupy, then there is a unique arrangement of the parcels (see Cullen (2006) for references). Each side of the polygons satisfies the Margules formula for the slope (dz/dx) of a frontal discontinuity surface i.e.

$$\frac{dz}{dx} = -\frac{f\theta_0[M]}{g[\theta]} \quad (2)$$

where $[\]$ indicates the jump in enclosed variable across the parcel boundary; θ_0 is a reference value of θ and g is the gravity acceleration. Algorithms for solving this essentially geometric construction problem have been developed by Simon Chynoweth (Cullen et al, 1985) and Jim Purser (the ‘panel-beater algorithm’ described in Cullen, 2006). For instance Fig. 2a shows a height section through a two-dimensional atmosphere at rest that has been represented by a regular array of parcels. The black parcel is given an increment of heat to raise its potential temperature substantially. In Fig. 2b we see the new equilibrium state after the parcel has convected to its neutral buoyancy level sandwiched between two layers of parcels for which its θ value is intermediate. The black parcel has now adopted a lens shape since inertial stability prevents it from spreading into a thin layer stretching across the domain. In the region where the black parcel originated the two neighbouring parcels that were at its side come together and form a strong cyclonic region with parcels above and below being sucked into the hole left behind. From the perspective of real convection the lens can be related to the circular cirrus outflow regions of Mesoscale Convective Systems (MCS) seen in satellite imagery. Movie loops confirm the anticyclonic sense rotation in the cloud and the very cold dome upper surface observed in MCSs is explained by the adiabatic cooling due to uplift during the creation of the lens.

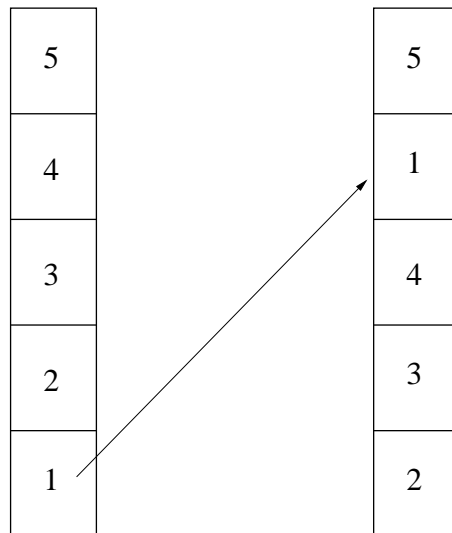


Figure 1: Equilibrium parcel configuration for a simple column atmosphere before (left) and after (right) parcel 1 has convected.

The above model of the convective jump problem is a fairly coarse discretization and it is possible to solve certain similar convective thought experiments by analytic methods (Shutts, 1987). Figure 3 is a schematic representation of the balanced end-state resulting from inviscid penetrative convection showing the lens/front features and associated velocity field. In this representation the convected air forms a region of constant M implying zero absolute vorticity (and also potential vorticity - hereafter the 'PV'). In the region from which the convected air has originated a vertical front is formed from air that bounded that region whilst conserved M as it collapsed inwards to form the vertical front. In this inviscid limit the front is a delta function in the PV field - similar to that appearing in the semi-geostrophic frontogenesis problem (Cullen and Purser, 1985).

It is possible to solve the convective jump problem for an initial state comprising uniform vertical shear flow in geostrophic and hydrostatic balance. The convecting parcel is then a two-dimensional infinite tube of air lying parallel to the vertical wind shear vector. Figure 4a shows the initial distribution of M and θ together with the region of air near the surface which is assumed to convect without mixing with the environment but with internal mixing homogenizing M and θ . The balanced final state has a lens displaced towards smaller x along the M surfaces. This is an example of penetrative *slantwise* convection - a process that may be observable in strong frontal zones although forced frontogenetic ascent usually makes the identification of slantwise convection difficult.

The circularly-symmetric version of convective jump thought experiment is considerably more difficult to solve but very interesting to contemplate. To investigate this Shutts et al (1988) transformed the x coordinate of the parcel model to a particular radial coordinate that makes the parcel boundaries straight. In this way gradient wind balance is observed rather than geostrophic balance and now parcel area conservation does not equate to continuity of mass. The experiment considers the convection of a cylinder of air in a rotating system. Unlike the 2D rectilinear problem where air either side of the parcel is brought together, here parcels are toruses and angular momentum conservation would prevent collapse onto the rotation axis since this would generate infinite wind speeds. Figure 5 summarises the form of the balanced flow structures implied by the Shutts et al study. Air in the cylinder is replaced by subsidence to the surface and inward converge onto a sloping, vase-shaped frontal surface. On the outer side of the surface there is a strong tangential wind which decays outwards. Within the region bounded by the surface the winds are light. In general the maximum radius of this hurricane-like eyewall is much smaller than the radius of the upper lens. The anticyclonic upper lens has its strongest tangential wind near the outer rim.

The above convective jump problem has clear relevance to the balanced flows that remain after mesoscale

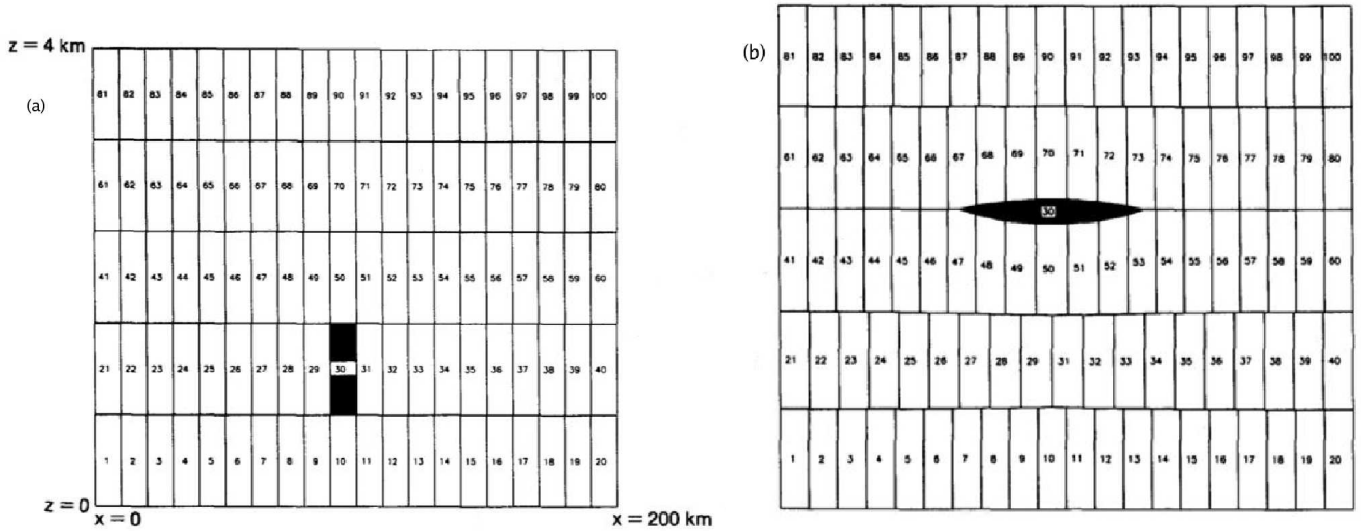


Figure 2: Equilibrium parcel configuration (left) before; (right) after the black parcel has convected for a 2D rectilinear flow. M is conserved for each parcel and lateral displacements cause the generation of v .

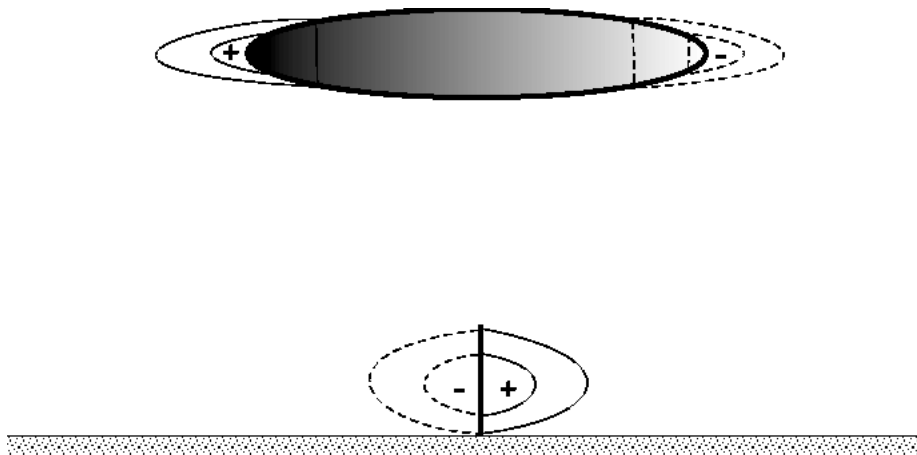


Figure 3: Schematic diagram showing the 2D lens and front structures resulting from penetrative convection together with associated velocity contours. The shading within the lens represents v with black representing the strongest flow into the picture and white the strongest flow out of the picture. If M is uniform within the lens then the $\zeta = -f$ and the potential vorticity is zero. The vertical front protruding from the ground has a discontinuity in v and therefore infinite potential vorticity.

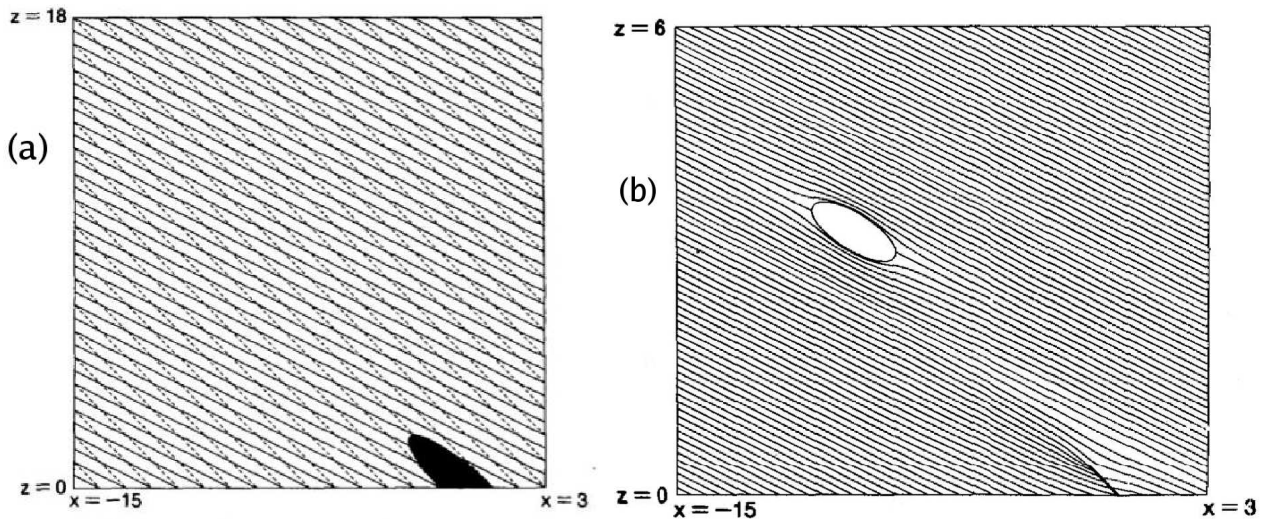


Figure 4: (a) Initial state for convective jump thought experiment showing θ contours (solid lines) and M contours (dashed lines). The black region is the air that will be assumed to convect. (b) The final state distribution of θ contours after the air in the black region has convected and formed an elliptical lens region of uniform θ (after internal mixing of the original θ values) (taken from Shutts, 1987). Note the differing vertical extent of figures (a) and (b).

convective system activity and also to hurricane dynamics. The picture is complicated somewhat by the effects of evaporation cooling which creates downdraughts that effectively raise the height from which mass is removed by convection. This leads to the formation of mid- to lower tropospheric meso-vortices as air converges into the region from which air convects.

In hurricanes, radial inflow of air in the lower troposphere leads to ascent close to the eyewall. Since equivalent potential temperature (θ_e) and angular momentum (M_a) are approximately conserved, gradient wind balance and hydrostatic balance can be shown to constrain the θ_e and M_a surfaces to the shape of a bath plug-hole vortex i.e.

$$h(r) = \left[\frac{M_a \theta(M_a)}{g \theta'(M_a)} \right] \frac{1}{r^2} + F(M_a) \quad (3)$$

where $h(r)$ is the height of the angular momentum surface with value M_a ; r is the radius; $\theta(M_a)$ is the functional dependence of θ on M_a with derivative $\theta'(M_a)$, and $F(M_a)$ is an arbitrary function (Shutts, 1981). Fig. 6 shows a cross-section through a dry, zero PV vortex showing its similarity to hurricane structure. Emanuel (1986) has used the zero moist PV assumption as the basis of his steady-state model of hurricanes in which latent heat energy from the sea drives slantwise-neutral ascent along the angular momentum surface.

In summary then, the parcel model and associated analytic theory has shown how deep, penetrative convection in a rotating environment can generate distinctive frontal and lens-like flow features characterized by singular and zero potential vorticity respectively. This type of convective frontogenesis is very powerful and would lead to wind shear-lines on the time scale of the convection itself. The lens-like structures formed by convective mass detrainment are identified with quasi-circular outflows of mesoscale convective systems with their pronounced anticyclonic vorticity and intense cold domes. High PV is embedded in mesoscale convective vortices which form in the effective mass sink region of MCSs in the lower troposphere. The magnitude and scale of the PV anomalies created by mesoscale convective systems are sufficiently large that they affect the development of baroclinic weather systems yet forecasting when and where MCSs will occur is a challenge. In other words there is an upscale cascade of energy from convection that reduces the predictability of the atmosphere.

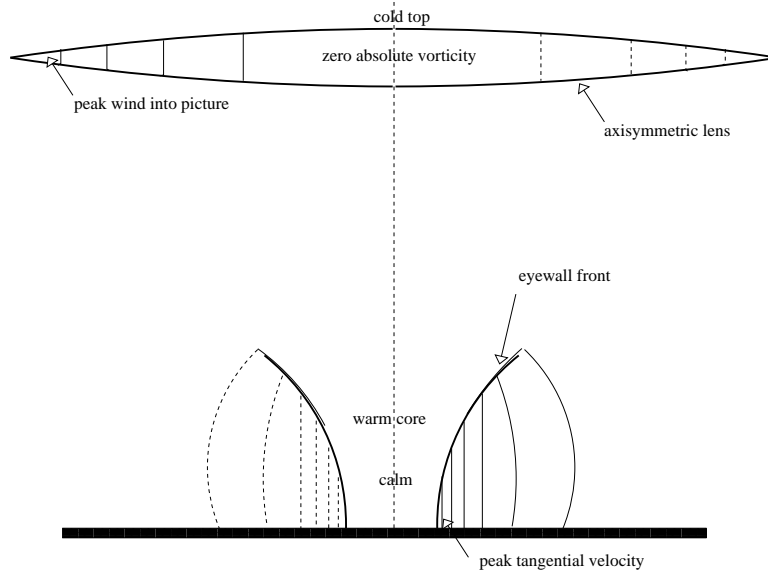


Figure 5: Radius-height section of the balanced tangential velocity distribution resulting from the convection of a cylindrical region of air in contact with the ground. Toroidal parcels are unable to contact to the origin conserving angular momentum so air gets sucked down to the surface and an outward-sloping 'eyewall' front is formed. The tangential velocity is maximized at the front and winds are light the other side of the front. Anticyclonic swirling flow is concentrated at the rim of an upper lens containing the convected air and weak outside. The figure was adapted from Figs. 3b and 4b of Shutts, Booth and Norbury (1988)

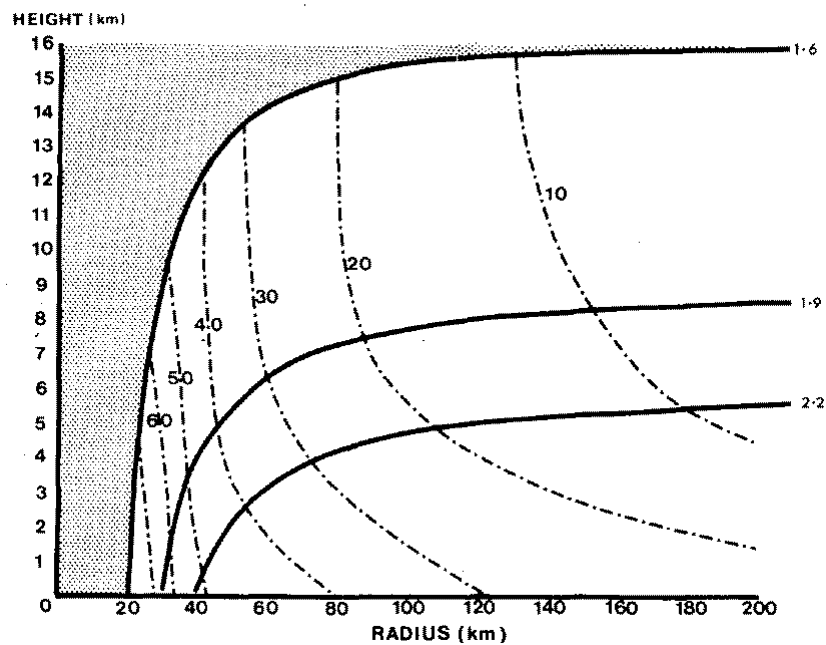


Figure 6: Vertical section through a zero PV model of a balanced hurricane flow. The shaded region corresponds to the eye and the thick solid lines are M_a and θ surfaces. The dash-dot lines are contours of tangential velocity in ms^{-1} and show a maximum near the surface at the eyewall (from Shutts, 1981)

3 Parametrization and effects of convection dynamics : equilibrium and stochastic

3.1 Cumulus friction

Convection parametrization is primarily concerned with the thermodynamic impacts of an ensemble of convective clouds whose collective action is to stabilize the atmosphere through heat and moisture transport. Momentum transfer can be regarded as a by-product of these transports. This is a similar situation to the role of large-scale baroclinic weather systems in the general circulation for which the accompanying poleward transport of westerly momentum.

In spite of the non-conservation of momentum for convecting air parcels, the net effect of convective updraughts and downdraughts in vertically-sheared flow is to cause downgradient transport of momentum and this has been parametrized as a mixing process (Schneider and Lindzen, 1977; Kershaw and Gregory, 1997). Using an axisymmetric model of the general circulation of the atmosphere Schneider and Lindzen suggest that the strength of the Hadley circulation is governed by the intensity of convective momentum transport. Effectively, downgradient momentum transport tends to destroy thermal wind balance and the eddy flux divergence of these Reynolds' stresses is balanced by a mean meridional circulation \bar{v} given by:

$$(f + \overline{\zeta})\bar{v} \approx S_u \quad (4)$$

where the overline denotes a zonal average and S_u is the eddy (westerly) momentum flux divergence (see Walker and Schneider, 2006). When $S_u > 0$ (i.e. eddies forcing easterly flow), a meridional flow is generated whose strength is inversely proportional to the absolute vorticity. In the upper branch of the Hadley circulation, $S_u > 0$ since deep convection brings air with lower westerly momentum into this region. This results in $v > 0$ since the absolute vorticity is positive for inertial stability and works in the sense of supporting the Hadley circulation.

In practice S_u is dominated by the meridional flux divergence of poleward momentum transport due to synoptic and planetary-scale eddies. This can be viewed as due to the influx of Rossby wave action that is radiated from maturing baroclinic weather systems and planetary waves forced by mountains and thermal land-sea contrast. Incoming wave packets effectively dump easterly momentum into the subtropics at upper tropospheric levels and the resulting westerly flow deceleration causes a poleward cross-isobaric flow.

3.2 Mesoscale PV anomaly generation

As seen in section 2, convective mass transfer can generate potential vorticity anomalies in the form of lens of very low PV and frontal structures characterized by very high PV. Mesoscale convective systems are of sufficient spatial extent that they may influence the development of baroclinic weather systems downstream and therefore undermine the predictability of the large-scale flow. Shutts and Gray (1994) carried out numerical simulations of the geostrophic adjustment process that followed the convective mass transfer due to a single plume in an idealized environment. They found that up to 30% of the kinetic energy generated by buoyancy forces could be 'captured' in balanced flow with associated lens-front PV anomalies. In contrast Schubert et al (1980) performed a linear analysis of the adjustment of a circular region following convective warming and concluded that in the absence of background rotation, the energy efficiency for producing balanced vortical motion was only a few percent. However they also showed that in presence of a pre-existing vortex the energy capture efficiency was much greater.

Shutts and Gray (1994) showed that in 2D, the amount of balanced energy (E) produced by convection increases as the square of the amount of mass convected (M_c). A simple scaling argument suggests that the kinetic energy of the lens is $(fr)^2 \times$ the lens volume where r is the lens radius and equal to the largest lateral displacement created by its expansion (fr is the velocity generated by Coriolis torque). The lens thickness scales as the

Rossby height $\frac{f}{N}r$ (where N is the buoyancy frequency) and if one assumes unit density, $M_c \sim \frac{f}{N}r^2$. Therefore the energy in the lens is given by

$$E \sim (fr)^2 \times M_c \sim fNM_c^2 \quad (5)$$

Now parcel theory says that the amount of kinetic energy generated by buoyancy forces is $CAPE \times M_c$ implying that the work required to expand the lens will eventually exceed that which can be provided by the convective available potential energy. Setting the balanced flow energy of the lens equal to the amount of kinetic energy released gives

$$E \sim fNM_c^2 = CAPE \times M_c \quad (6)$$

or

$$M_c = \frac{CAPE}{fN}. \quad (7)$$

Expressing M_c in terms of a maximum permissible lens radius r_* it follows that:

$$r_* = \frac{\sqrt{CAPE}}{f}. \quad (8)$$

One may regard this as a characteristic scaling for mesoscale convective system anvils and choosing $CAPE = 1000 \text{ J.kg}^{-1}$ and $f = 10^{-4} \text{ s}^{-1}$, $r_* \sim 300 \text{ km}$. Note that in the above argument it has been implicitly assumed that the available potential energy of the lens is equal to its kinetic and a factor of one half has been dropped from definition of kinetic energy.

The above results strictly only hold for a 2D rectilinear lens (e.g. no functional dependence on y in a Cartesian system). Gray (1998) developed this approach for axisymmetric lens and argued that the balanced flow energy should depend on $M_c^{5/3}$ rather than M_c^2 . He also showed that for a given amount of convective mass transfer, more balanced flow energy is created for a single plume than for the equivalent mass transfer split over many smaller plumes.

Another relevant length scale is the Rossby deformation radius (L_R) based on the depth of the convection (H_c) such that:

$$L_R = \frac{NH_c}{f}. \quad (9)$$

and with $H_c = 10 \text{ km}$ one finds $L_R = 1000 \text{ km}$. Therefore one might suppose that subsidence suppresses convection over a region 1000 km from an intense mesoscale convective system whose outflow ‘anvil’ may be about 600 km in diameter. Clearly these numbers, derived from scaling arguments, are only meant to be suggestive of what one might see in reality. They are, however, consistent with the observed size and spacing of mesoscale convective systems seen over Europe in summer - typically on the hot side of an approaching frontal trough.

Convection parametrization schemes are usually based on the concept of an ensemble of convective plumes in quasi-equilibrium with large-scale forcing. The explosive growth of mesoscale convective systems over the course of six hours does not fit that paradigm yet is poorly represented in most current global forecast models. Gray (2001) investigated the effect of PV anomalies - representative of those created by MCSs - on NWP forecasts. Depending on their location relative to baroclinic zones, a significant impact on downstream development was possible. Given the inherent uncertainty in knowing where MCSs will develop and their potential impact on forecast model error, a stochastic representation of their dynamical impact in ensemble prediction systems is suggested. Indeed the Met Office MOGREPS ensemble prediction system incorporates a ‘stochastic convective vorticity’ parametrization based on the earlier work of Gray (Bowler et al, 2008).

3.3 Upscale energy cascade

Convection in the atmosphere is a truly multi-scale phenomenon spanning length scales from tens of metres to hundreds of kilometres (scales less than 10 metres will be regarded as turbulence). In a direct numerical simulation of deep convection in a horizontally-periodic box of side 300 km Vallis et al (1997) showed that the resulting horizontal kinetic energy spectrum approximately followed a power law with $-5/3$ slope. They showed that both background rotation and vertical wind shear in the boundary layer assist in cascading energy to large scales though with the latter dominating. This is because ambient vorticity helps diabatic processes in convection create PV anomalies which subsequently participate in an upscale energy cascade. The mechanism by which energy reached the largest scales in the domain was apparently not an inverse quasi-2D energy cascade of the type proposed by Lilly (1983) (see Shutts and Gray, 1999). Rather, it seemed to appear simultaneously with the emergence of large-scale organization of the convection into long convergence lines with ≈ 60 km separation.

Being confined to a 300 km box, the Vallis et al simulation is unable to address the cascade of energy to the synoptic and planetary scales that is believed to occur in the tropical atmosphere. Even with the increasing in computing power ten years after that work it is still computationally prohibitive to repeat the simulation with a domain that spans the tropics. As a compromise, Shutts (2008) used a horizontally-anisotropic grid with about 16 times finer resolution in the east-west direction compared to the north-south. Also, the Coriolis parameter was made a linear function of y giving equatorial beta-plane geometry and a meridionally-varying sea surface temperature was incorporated. Specifically the domain was about 40,000 km in the east-west direction (about equal to the circumference of the Earth); 5000 km north-south and 30 km deep. The model was initialized with a constant easterly wind of 5 ms^{-1} and a vertical profile of temperature and humidity adapted from a tropical radiosonde ascent. Small random perturbations were added to initiate convection. Fig. 7 shows a time-height section of u at some point on the equator. Within a few days one can see waves with descending phase lines in stratosphere and as these amplify their period progressively increases. In the troposphere the waves have a longer vertical wavelength (≈ 10 km) and exhibit something closer to standing wave structure.

The u and v components of the wind were expanded in a Fourier series in x (with Gaussian structure in y) at all levels and the associated kinetic energy in each mode summed in the vertical. Fig. 8 shows these zonal wavenumber decompositions as a function of time. It is striking how wave energy across all wavenumbers appears near day 6 although concentrated in particular modes e.g. wavenumbers 4,6 and 10 for u . The rather limited time series of data from the model (15.4 days) can be decomposed spectrally and plots of kinetic energy density can be plotted as a function of zonal wavenumber and frequency. Fig. 9 shows such a decomposition for u and v when projected onto modes with Gaussian structure about the equator. The very different distributions of energy in u and v is partially explained by reference to the different dispersive properties of equatorially-trapped waves (Gill, 1982; Wheeler and Kiladis, 1999). The kinetic energy contribution from u is mainly in the form of equatorially-trapped Kelvin waves with a phase speed close to 18 ms^{-1} whereas the v contribution is in the form of a mixed Rossby-gravity wave.

In the model simulation at least, kinetic energy can be released in convective storms at the 10 km scale and migrated to low planetary wavenumbers in a mere six days. By the same token, long waves in the tropics organize the convection into cloud clusters and it is in this sense that tropical convection is ‘multi-scale’. The kinetic energy spectrum in these tropical experiments tends to be close to a $-5/3$ power law in wavenumber i.e. much flatter than the -3 power law that characterizes the planetary to mesoscales of middle latitudes.

4 Stochastic convective parametrization

Convection parametrization is usually formulated so as to provide the ensemble-average forcing effect of an assumed population of sub-gridscale clouds. For deep convection on current NWP grids with horizontal gridlengths of 25 to 50 km the ensemble-average convective tendency will be a poor estimate of the instantaneous

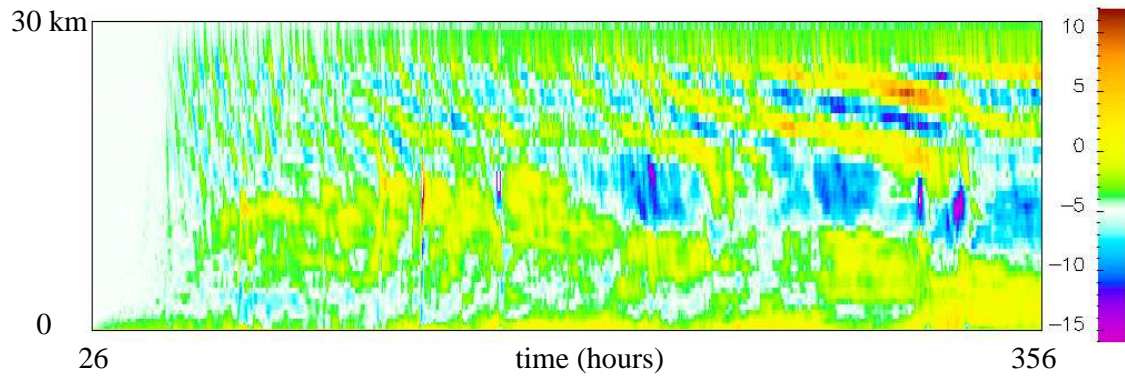


Figure 7: Time-height section of zonal wind at a point on the equator

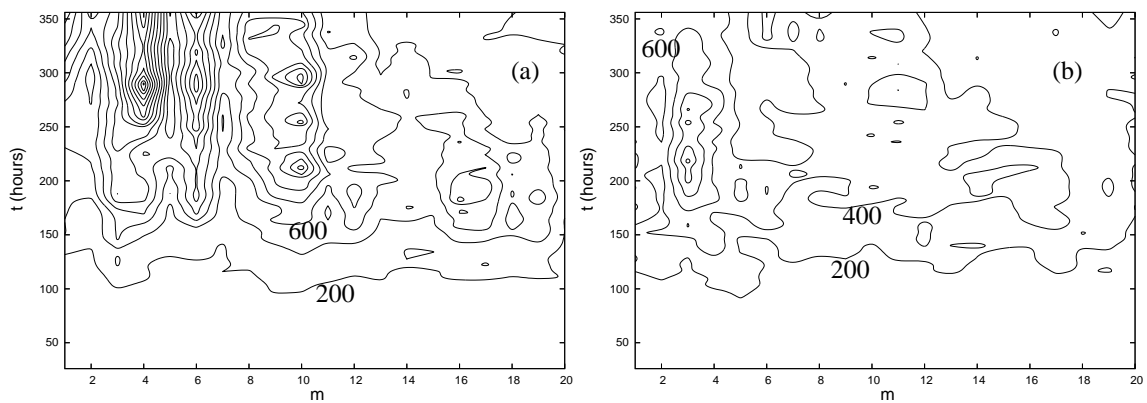


Figure 8: Total depth-integrated kinetic energy $\frac{1}{2y_1} \int_{-y_1}^{y_1} \int \frac{1}{2} \rho_0 (u^2 + v^2) dz dy$ in wavenumbers 1 to 20 versus time. $y_1 = 850$ km and the contour interval is 200 Jm^{-2} .

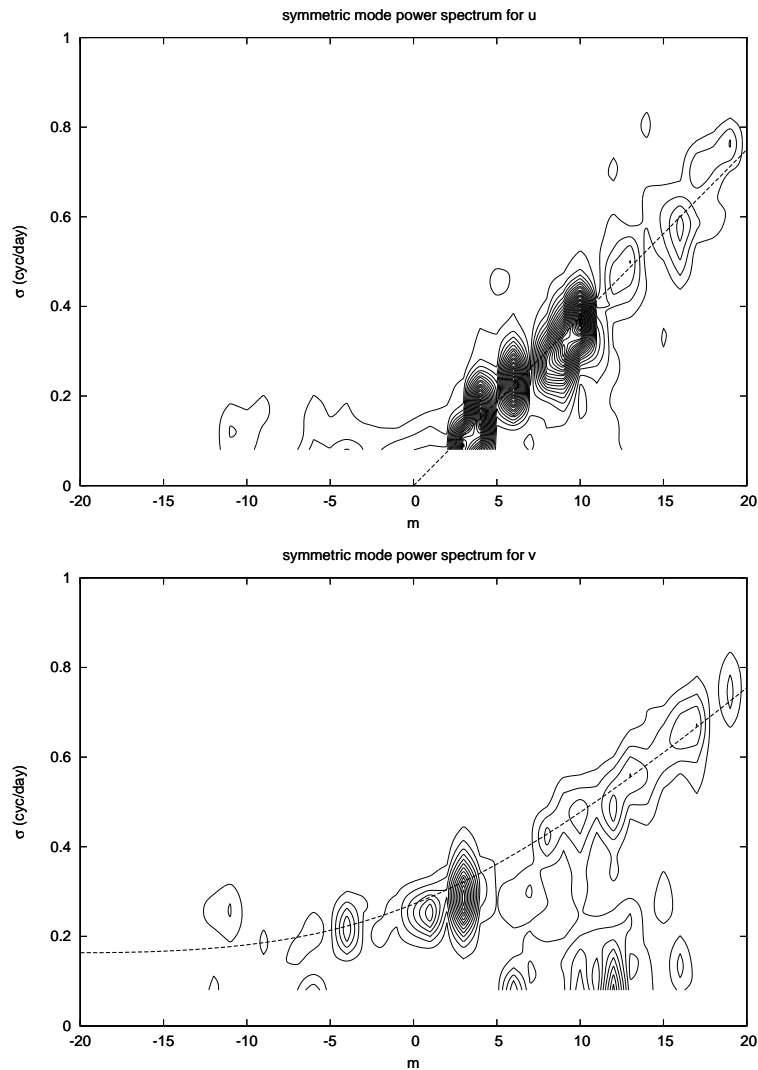


Figure 9: Height-averaged power in the symmetric component of u (upper) and v (lower) as a function of zonal wavenumber (m) and frequency (in cycles per day). Contour interval: $0.3 \text{ m}^2 \text{ s}^{-2}$. The dashed line in the upper plot corresponds to the Kelvin wave dispersion formula with an equivalent depth of 37 m, and that in the lower plot corresponds to the dispersion curve for the mixed Rossby-gravity wave with equivalent depth 33.8 m and an assumed background easterly wind of 3 m s^{-1} (obtained by applying a least squares curve fitting technique for $-12 < m < 20$ and excluding points with frequency less than 0.13 cycles/day).

thermodynamic tendency. However it is probably true to say that there is a tendency to focus on the worst case scenario (horizontally-uniform forcing) when considering the degree of uncertainty in predicting the location and intensity of convection. Quasi-balanced flow dynamics and certain gravity wave dynamical processes, orography and land-sea surface characteristics all have a strong influence on the likelihood of convection.

In the context of ensemble prediction systems and the representation of model error, Buizza et al (1999) introduced a simple technique for introducing stochastic fluctuations into NWP parametrizations. Their method (see also Palmer 2001) involves multiplying parametrization tendencies by a random number drawn from a uniform probability distribution function with a range between 0.5 and 1.5. Space and time correlation is introduced by using the same random number in latitude/longitude boxes larger than the underlying model grid and holding the number fixed for over a certain number of time steps. Each forecast member has a different set of random numbers and this helps to correct a universal deficiency in current EPS systems - lack of spread. Buizza et al. adjusted the size of the boxes and time interval over which the random numbers are held constant in order to tune this *stochastic physics* scheme to get the best skill. Optimal skill in the ECMWF ensemble prediction system (as measured by the Brier skill score for instance) was obtained for 10 latitude/longitude boxes and 6-h time intervals.

Lin and Neelin (2000, 2002) also experimented with stochastic perturbations to aspects internal to convective parametrization algorithms. More generally, Palmer (2001, 2006) proposed that representation of unresolved scales should be made using computationally efficient nonlinear stochastic-dynamic models, for example, based on cellular automata (CA). Specific examples using such an approach have been proposed, for example, based on the Ising model (Majda and Khouider 2002; Khouider et al. 2003) and a specific CA onto which stochastically backscattered convectively forced fields are projected (Shutts 2005).

Craig and Cohen (2006) use a statistical mechanics approach to determining probability distribution functions (hereafter called *pdf*) for individual cloud mass fluxes and areal-mean mass fluxes. Their theory requires many assumptions that are difficult to justify or are not true in real situations (e.g. no interaction between neighbouring clouds) yet it stands as the only published work that attempts to predict the character of the pdfs from first principles. It is shown how the individual cloud mass fluxes should follow an exponential (Boltzmann) distribution function and cloud-resolving model simulations support this prediction (Cohen and Craig, 2006). Craig and Cohen derive a pdf for an ensemble of clouds in which the total cloud-system mass flux is able to fluctuate in the sense of an ‘open system’. Using the results of this work Plant and Craig (2008) have designed a stochastic parametrization and implemented it in the Met Office Unified Model single column model.

In order to better characterize the pdfs of convective forcing Shutts and Palmer (2007) analysed a ‘big-domain’ cloud-resolving model simulation of tropical convection using a coarse-graining strategy. Their focus was on the pdf of the total diabatic tendency computed on a coarse grid and conditionally-sampled using a convective parametrization scheme. Using the coarse-grained model fields as input to the convection parametrization coarse grid columns could be grouped into different ranges of convective warming rates. Pdfs of the coarse-grained diabatic tendencies for each of these groups were then computed to give some idea of how the pdfs change as a function of the strength of parametrized convective warming. Figure 10a (taken from Shutts and Palmer, ‘2007) shows that considerable spread exists even for the large subset of coarse model columns for which the convective parametrization implies no convection (or very weak convection). For successively higher values of parametrized convective warming the mode of the pdf moves to higher diabatic tendencies as it should.

The dependence of the standard deviation of the diabatic tendency within a coarse box on the corresponding mean is plotted in Fig. 11 for various coarse-graining resolutions. Consistent with the assumptions underlying the ECMWF stochastic physics scheme, the relationship is linear yet the curves do not pass through the origin. Shutts and Palmer (2007) attributed this to a balance between latent heating and cooling associated with condensation/freezing and evaporation/melting respectively within coarse boxes. For reference only, the thin, dotted line in Fig. 11 is the relationship implied by the operational ECMWF stochastic physics scheme for 10 degree latitude/longitude boxes.

The spectral backscatter technique described by Berner et al (2008) is an adaption (for NWP) of the Large-Eddy

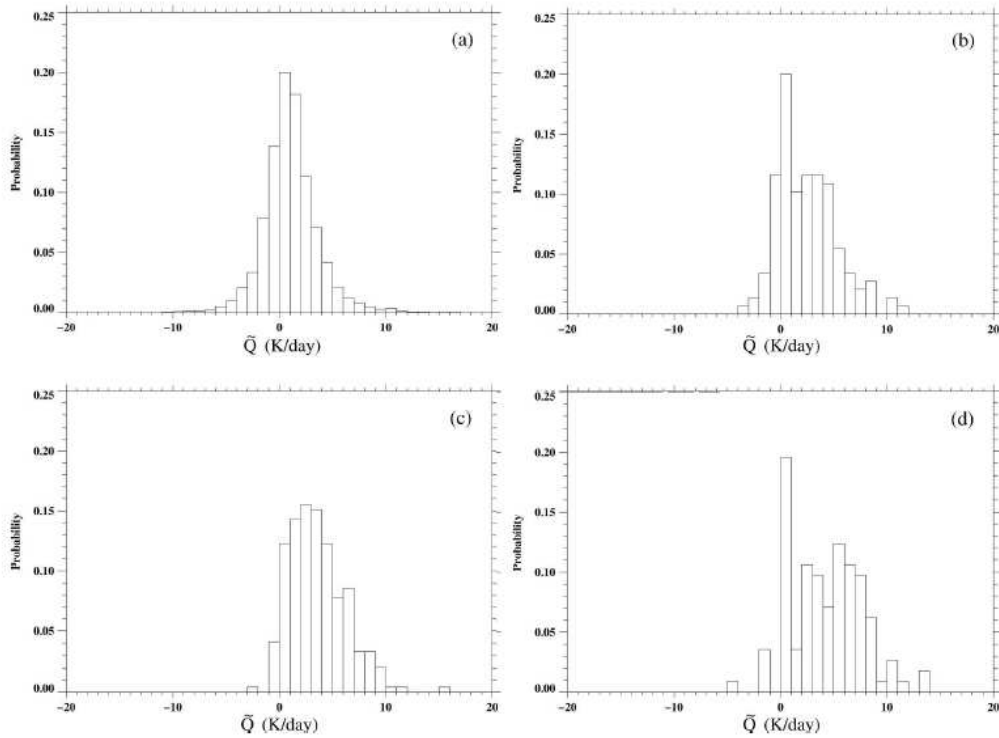


Figure 10: Probability distribution functions of the coarse-grained diabatic tendency (computed on a 320 km) grid conditioned on 4 different ranges of parametrized convective warming: (a) -0.1 to 0.1 K/day; (b) 0.1 to 10 K/day (c); 10 to 20 K/day and 20 to 40 K/day. (from Shutts and Palmer, 2007)

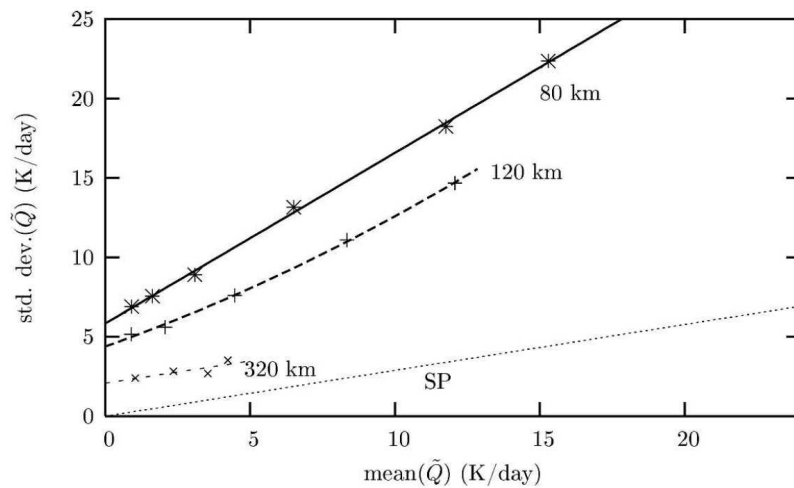


Figure 11: Dependence of the standard deviation of the coarse-grained diabatic tendency on its mean value within specified ranges of the parametrized convective warming. Coarse-box sizes are given as labels next to the appropriate curves. The thin dotted line corresponds to the relationship between the mean and standard deviation of parametrized warming implied by the ECMWF stochastic physics scheme.(from Shutts and Palmer, 2007)

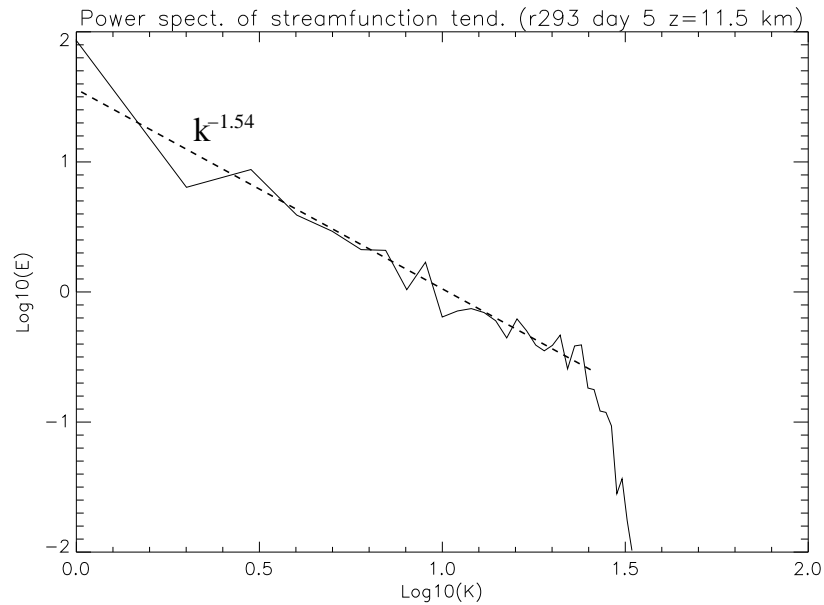


Figure 12: Spectral power in the streamfunction forcing at a height of 11.5 km and on day 5 of the cloud-resolving model simulation described by Shutts and Palmer (2007). The $\log_{10}(K)$ axis represents the logarithm (base 10) of the integer wavenumber so that wavenumber one represents wavelength equal to the box dimension of 7680 km.

Simulation (LES) method proposed by Mason and Thomson (1992) and follows an earlier implementation using a cellular automaton pattern generator (Shutts, 2005). The adaption of Mason and Thomson's 3D turbulent backscatter has three elements to it:

- it is quasi-two-dimensional with their vector potential-based momentum forcing being replaced by a streamfunction forcing
- its dissipation rate calculation is based on a combination of numerical, gravity/mountain drag and convective dissipation rather than eddy viscosity dissipation alone
- it uses a spectral pattern generator instead of smoothed random numbers with each spectral component evolving smoothly as first-order auto-regressive process.

The mean spectral power distribution for the streamfunction forcing is assumed to follow a power law in wavenumber and was calibrated using the coarse-graining procedure described in Shutts and Palmer (2007) as applied to momentum tendency. The computed streamfunction forcing power spectrum (Fig. 12) supports the power law assumption with an exponent of ~ -1.54 . The strength of the streamfunction forcing is modulated by the square root of the dissipation rate whose convective component is determined from the product of a diagnosed convective updraft kinetic energy and the mass detrainment rate. Berner et al (2008) demonstrate that the use of the backscatter scheme provides increased spread to the ECMWF ensemble prediction system and with it, improved probability skill scores.

5 Conclusion

Whilst deep convection is an unresolved process on current global forecast model grids its cloud population density is too low for the instantaneous mass fluxes to be represented by an equilibrium, ensemble-mean value such as provided by convection parametrization. Non-equilibrium statistical fluctuations take the form of mesoscale

convective systems that are associated with potential vorticity anomalies and accompanying balanced flows. They also excite inertia-gravity waves whose action in the tropics is to organize the subsequent convection. Large-scale flow deformation in synoptic weather systems strains convectively-generated PV anomalies into filaments and forces an upscale energy cascade. Stochastic kinetic energy backscatter schemes currently under development contain a component that represents this redistribution of convectively-generated kinetic energy to the resolved flow.

As with conventional convective parametrization, future development of stochastic techniques needs to be based on concrete scientific findings e.g. coarse-grained statistics from big-domain cloud-resolving models. Remotely-sensed observations and statistical theories will also have a big part to play in designing stochastic algorithms for use in NWP and climate models. Ultimately though there is a danger of overstating the degree to which convective-scale phenomena destroy predictability. Balanced flow systems and topographic influences (terrain height and surface type) provide strong controls over when and where deep convection will break out. Recent improvements in convective parametrization at ECMWF (see the paper by P. Bechtold in this volume) show that modified algorithms breaking the quasi-equilibrium assumption can markedly improve model performance without being inherently stochastic. One should therefore keep an open mind as to the degree to which stochastic parametrization will be needed.

6 References

- Baldwin, M., L.J.Gray, T.J. Dunkerton, K. Hamilton, P.H. Haynes, W.J. Randel, J.R. Holton, M.J. Alexander, I. Hirota, T. Horinouchi, D.B.A. Jones, J.S. Kinnersley, C. Marquardt, K. Sato and M. Takahashi (2001) The Quasi-Biennial Oscillation. *Reviews of Geophysics*, **39**, 179-229.
- Berner, J., G.J Shutts, M. Leutbecher and T.N. Palmer (2008) A spectral stochastic kinetic energy backscatter scheme and its impact on flow-dependent predictability in the ECMWF ensemble prediction system. *J. Atmos. Sci.* (accepted).
- Bjerknes, J. (1938) Saturated-adiabatic ascent of air through dry-adiabatically descending environment. *Q. J. R. Meteorol. Soc.*, **64**, 325-330.
- Bowler, N., A. Arribas, K R. Mylne, K.B. Robertson, S.E. Beare (2008) The MOGREPS short-range ensemble prediction system. *Q.J.R. Meteorol. Soc.*, **134**, 703 - 722.
- Browning, K.A. and F.H. Ludlam (1962) Airflow in convective storms. *Q.J.R. Meteorol. Soc.*, **88**, 117-135.
- Buizza R., M. Miller, and T. N. Palmer, 1999: Stochastic representation of model uncertainty in the ECMWF ensemble prediction system. *Q. J. R. Meteorol. Soc.*, **125**, 2887-2908.
- Craig, G.C. and B.G Cohen (2006) Fluctuations in an Equilibrium Convective Ensemble. Part I: Theoretical Formulation. *J. Atmos. Sci.*, **63**, 1996-2004.
- Cohen, B.G. and G.C. Craig (2006) Fluctuations in an Equilibrium Convective Ensemble. Part II: Numerical Experiments. *J. Atmos. Sci.*, **63**, 2005-2015.
- Cullen, M.J.P. (2006) Mathematical Theory of Large-Scale Atmosphere/Ocean Flow. *Imperial College Press*, 259pp.
- Cullen, M.J.P., S. Chynoweth and R.J. Purser (1985) On semi-geostrophic flow over synoptic-scale topography. *Q. J. R. Meteorol. Soc.*, **113**, 163-180.
- Cullen, M.J.P. and R.J. Purser (1984) An Extended Lagrangian Theory of Semi-Geostrophic Frontogenesis. *J. Atmos. Sci.*, **41**, 1477-1497.
- Emanuel, K. (1986) An Air-Sea Interaction Theory for Tropical Cyclones. Part I: Steady-State Maintenance. *J. Atmos. Sci.*, **43**, 585-605.

- Gough, D.O. and D. Lynden-Bell (1968) Vorticity expulsion by turbulence : astrophysical implications of an Alka-Seltzer experiment. *J. Fluid Mechs.*, **32**, 437-447.
- Gill, A.E. (1982) Atmosphere-Ocean Dynamics. *International Geophysics Series Vol. 30, Academic Press.*,
- Gray, M.E.B. (1998) An investigation into convectively generated potential-vorticity anomalies using a mass-forcing model. *Q.J.R. Met.Soc.*, **125**, 1589 - 1605.
- Gray, M.E.B. (2001) The impact of mesoscale convective-system potential-vorticity anomalies on numerical-weather-prediction forecasts. *Q.J.R. Met.Soc.*, **127**, 73-88.
- Kershaw, R. and D. Gregory (1997) Parametrization of momentum transport by convection I: Theory and cloud modelling results. *Q.J.R. Met.Soc.*, **123** , 1133-1151.
- Khouider B., A. J. Majda, and M. A. Katsoulakis (2003) Coarse-grained stochastic models for tropical convection and climate. *Proc. Natl. Acad. Sci. USA*, **100**, 11941-11946.
- Korty, R.L and T. Schneider (2007) A Climatology of the Tropospheric Thermal Stratification Using Saturation Potential Vorticity. *J. Climate*, **20**, 5977-5991.
- Lilly, D.K. (1983) Stratified Turbulence and the Mesoscale Variability of the Atmosphere. *J. Atmos. Sci.*, **40**, 749-761.
- Lin J.-B. and J. Neelin (2000) Influence of a stochastic moist convective parametrization on tropical climate variability. *Geophys. Res. Lett.*, **27**, 3691-3694.
- Lin J.-B., and J. Neelin (2002) Considerations for stochastic convective parametrization. *J. Atmos. Sci.*, **59**, 959-975.
- Majda, A.J. and B. Khouider (2002) Stochastic and mesoscopic models for tropical convection. *Proc. Natl. Acad. Sci. USA*, **99**, 1123-1128.
- Mason, P. J. and D. J. Thomson (1992) Stochastic backscatter in large-eddy simulations of boundary layers. *J. Fluid Mech.*, **242**, 51-78.
- Moncrieff, M.W. and J.S.A. Green (1972) The propagation and transfer properties of steady convective overturning in shear. *Q.J.R. Meteorol. Soc.*, **98**, 336-352.
- Moncrieff, M.W.(1981) A theory of organized steady convection and its transport properties. *Q.J.R. Meteorol. Soc.*, **107**, 29-50.
- Moncrieff, M.W.(1992) Organized convective systems: Archetypal dynamical models, mass and momentum flux theory, and parametrization. *Q.J.R. Meteorol. Soc.*, **118**, 819-850.
- Montgomery, M. T., and R. J. Kallenbach, 1997: A theory for vortex Rossby waves and its application to spiral bands and intensity changes in hurricanes. *Quart. J. Roy. Meteor. Soc.*, **123**, 435-465.
- Palmer, T. N. (2001). On parametrizing scales that are only somewhat smaller than the smallest resolved scales, with application to convection and orography. *ECMWF Workshop on New Insights and Approaches to Convective Parametrization, 4-7 November 1996. Shinfield, Reading, UK*
- Palmer, T.N. (2006) Predictability of weather and climate: from theory to practice. *Predictability of Weather and Climate*, Ed. T.N. Palmer and R. Hagedorn. Cambridge University Press. DOI: 10.2277/0521848822.
- Plant, R.S. and G.C. Craig (2008) A Stochastic Parameterization for Deep Convection Based on Equilibrium Statistics. *J. Atmos. Sci.*, **65**, 87-105.
- Schneider, E.K. and R.S. Lindzen (1977) Axially Symmetric Steady-State Models of the Basic State for Instability and Climate Studies. Part I. Linearized Calculations. *J. Atmos. Sci.*, **34**, 263-279.
- Schubert, W.H., J. Hack, P.L. Silva Dias, and S.R. Fulton (1980) Geostrophic Adjustment in an Axisymmetric

- Vortex. *J. Atmos. Sci.*, **37**, 1464-1484.
- Scorer, R. S., (1966) Origin of cyclones. *Sci.J.*, **2**, 46-52.
- Shutts, G.J. (1981) Hurricane Structure and the Zero Potential Vorticity Approximation. *Mon. Wea. Rev.*, **109**, 324-329.
- Shutts, G.J. (1987) Balanced Flow States Resulting from Penetrative, Slantwise Convection. *J. Atmos. Sci.*, bf 44, 3363-3376.
- Shutts, G.J., M. Booth and J. Norbury (1988) A Geometric Model of Balanced, Axisymmetric Flows with Embedded Penetrative Convection. *J. Atmos. Sci.*, bf 45, 2609-2621.
- Shutts, G.J. and M.E.B. Gray (1994) A numerical modelling study of the geostrophic adjustment process following deep convection. *Q.J.R. Meteorol. Soc.*, **120**, 1145 - 1178.
- Shutts, G.J. and M.E.B. Gray (1999) Numerical simulations of convective equilibrium under prescribed forcing. *Q.J.R. Meteorol. Soc.*, **125**, 2767-2787.
- Shutts G.J. (2005) A kinetic energy backscatter algorithm for use in ensemble prediction systems. *Q.J.R. Meteorol. Soc.*, **131**, 3079-3102.
- Shutts, G.J. and T.N. Palmer (2007) Convective Forcing Fluctuations in a Cloud-Resolving Model: Relevance to the Stochastic Parameterization Problem. *J. Climate*, **20**, 187-202.
- Shutts, G.J. (2008) The forcing of large-scale waves in an explicit simulation of deep tropical convection. *Dyn. Atmos. Oceans*, **45**, 1-25.
- Vallis, G.K., G. J. Shutts and M. E. B. Gray (1997) Balanced mesoscale motion and stratified turbulence forced by convection. *Q.J.R. Meteorol. Soc.*, **123**, 1621-1652.
- Walker, C.C. and T. Schneider (2006) Eddy influences on Hadley Circulations: Simulations with an idealized GCM. *J. Atmos. Sci.*, **63**, 3333-3350.
- Wheeler, M. and G. N. Kiladis (1999) Convectively Coupled Equatorial Waves: Analysis of Clouds and Temperature in the Wavenumber-Frequency Domain. *J. Atmos. Sci.*, **56**, 374-399.